

# Cortical patterning of abnormal morphometric similarity in psychosis is associated with brain expression of schizophrenia-related genes

Sarah E Morgan<sup>a,1</sup>, Jakob Seidlitz<sup>a,b</sup>, Kirstie J Whitaker<sup>a,c</sup>, Rafael Romero-Garcia<sup>a</sup>, Nicholas E Clifton<sup>d,e</sup>, Cristina Scarpazza<sup>f,g</sup>, Therese van Amelsvoort<sup>h</sup>, Machteld Marcelis<sup>h</sup>, Jim van Os<sup>h</sup>, Gary Donohoe<sup>i</sup>, David Mothersill<sup>i</sup>, Aiden Corvin<sup>j</sup>, Andrew Pocklington<sup>e</sup>, Armin Raznahan<sup>b</sup>, Philip McGuire<sup>f</sup>, Petra E Vértes<sup>a,c,k,2</sup>, and Edward T Bullmore<sup>a,1,2</sup>

<sup>a</sup>Department of Psychiatry, University of Cambridge, Cambridge CB2 0SZ, UK; <sup>b</sup>Developmental Neurogenetics Unit, National Institute of Mental Health, Bethesda, MD 20892, USA; <sup>c</sup>The Alan Turing Institute, London, NW1 2DB, UK; <sup>d</sup>Neuroscience and Mental Health Research Institute, Cardiff University, Cardiff, UK; <sup>e</sup>MRC Centre for Neuropsychiatric Genetics and Genomics, Institute of Psychological Medicine and Clinical Neurosciences, Cardiff University, Cardiff, UK; <sup>f</sup>Department of Psychosis Studies, Institute of Psychiatry, Psychology and Neuroscience, King's College London, London SE5 8AF, UK; <sup>g</sup>Department of General Psychology, University of Padova, 35131 Padova, Italy; <sup>h</sup>Maastricht University, Maastricht, The Netherlands, 616 6200 MD; <sup>i</sup>School of Psychology, NUI Galway, Galway, Ireland, H91 TK33; <sup>j</sup>Department of Psychiatry, Trinity College Dublin, Dublin 8, Ireland; <sup>k</sup>School of Mathematical Sciences, Queen Mary University of London, London E1 4NS, United Kingdom; <sup>1</sup>GlaxoSmithKline R&D, Stevenage SG1 2NY, UK

This manuscript was compiled on March 25, 2019

1 **Schizophrenia has been conceived as a disorder of brain connect-**  
2 **ivity but it is unclear how this network phenotype is related to the**  
3 **underlying genetics. We used morphometric similarity analysis of**  
4 **magnetic resonance imaging (MRI) data as a marker of inter-areal**  
5 **cortical connectivity in three prior case-control studies of psychosis:**  
6 **in total, N=185 cases and N=227 controls. Psychosis was associated**  
7 **with globally reduced morphometric similarity (MS) in all 3 studies.**  
8 **There was also a replicable pattern of case-control differences in**  
9 **regional MS which was significantly reduced in patients in frontal**  
10 **and temporal cortical areas, but increased in parietal cortex. Using**  
11 **prior brain-wide gene expression data, we found that the cortical**  
12 **map of case-control differences in MS was spatially correlated with**  
13 **cortical expression of a weighted combination of genes enriched**  
14 **for neurobiologically relevant ontology terms and pathways. In**  
15 **addition, genes that were normally over-expressed in cortical areas**  
16 **with reduced MS were significantly up-regulated in three prior post**  
17 **mortem studies of schizophrenia. We propose that this combined**  
18 **analysis of neuroimaging and transcriptional data provides new**  
19 **insight into how previously implicated genes and proteins, as well**  
20 **as a number of unreported genes in their topological vicinity on**  
21 **the protein interaction network, may drive structural brain network**  
22 **changes mediating the genetic risk of schizophrenia.**  
23

dysconnectivity | network neuroscience | psychosis | morphometric similarity | Allen Human Brain Atlas

1 **P** psychotic disorders have a lifetime prevalence of 1-3% and  
2 can be extremely debilitating. However, despite significant  
3 efforts, the brain architectural changes and biological  
4 mechanisms causing psychotic disorders are not yet well  
5 understood and there has been correspondingly limited progress  
6 in the development of new therapeutics.

7 Magnetic resonance imaging (MRI) studies of schizophrenia  
8 have robustly demonstrated local structural differences in  
9 multiple cortical areas, subcortical nuclei and white matter tracts  
10 (1). The most parsimonious explanation of this distributed,  
11 multicentric pattern of structural change is that it reflects  
12 disruption or dysconnectivity of large-scale brain networks  
13 comprising anatomically connected brain areas. However, test-  
14 ing this dysconnectivity hypothesis of psychotic disorder has  
15 been constrained by the fundamental challenges in measuring  
16 anatomical connectivity and brain anatomical networks in

humans. The principal imaging methods available for this  
purpose are tractographic analysis of diffusion weighted imag-  
ing (DWI) and structural covariance analysis of conventional  
MRI. DWI-based tractography generally under-estimates the  
strength of long distance anatomical connections, for example  
between bilateral homologous areas of cortex. Structural cov-  
ariance analysis is not applicable to single subject analysis  
and its biological interpretation is controversial (2).

We recently proposed a technique known as “morphometric  
similarity mapping” (3), which quantifies the similarity  
between cortical areas in terms of multiple MRI parameters  
measured at each area and can be used to construct whole  
brain anatomical networks for individual subjects. In keeping  
with histological results indicating that cytoarchitectonically  
similar areas of cortex are more likely to be anatomically  
connected (4), morphometric similarity (MS) in the macaque  
cortex was correlated with tract-tracing measurements of ax-  
onal connectivity. Compared to both tractographic DWI-based

## Significance Statement

Despite significant research, the biological mechanisms underlying schizophrenia are still unclear. We shed fresh light on structural brain differences in psychosis using a new approach called morphometric similarity mapping, which quantifies the structural similarity between brain regions. Morphometric similarity was globally reduced in psychosis patients in three independent datasets, implying that patients' brain regions were more differentiated from each other, less interconnected. Similarity was especially decreased in frontal and temporal regions. This anatomical pattern was correlated with expression of genes enriched for nervous system development and synaptic signaling, and genes previously associated with schizophrenia and anti-psychotic treatments. So we begin to see how combining genomics and imaging can give a more integrative understanding of schizophrenia, which might inform future treatments.

E.T.B. is employed half-time by the University of Cambridge and half-time by GlaxoSmithKline; he holds stock in GSK.

<sup>2</sup>P.E.V. and E.T.B. contributed equally to this work.

<sup>1</sup>To whom correspondence should be addressed. E-mail: sem91@cam.ac.uk

35 networks and structural covariance networks, MS networks  
36 included a greater proportion of connections between human  
37 cortical areas of the same cytoarchitectonic class. Individual  
38 differences in regional mean MS, or “hubness” of cortical nodes  
39 in MS networks, accounted for about 40% of the individual differ-  
40 ences in IQ in a sample of 300 healthy young people. These  
41 results suggest that MS mapping could provide a useful new  
42 tool to analyse psychologically relevant biological differences  
43 in brain structure.

44 Here we used MS mapping to test the dysconnectivity hy-  
45 pothesis of psychosis in three independent case-control MRI  
46 datasets: the Maastricht GROUP study (83 cases, 68 controls)  
47 and the Dublin study (33 cases and 82 controls), both made  
48 available as legacy datasets for the PSYSCAN project, and the  
49 publicly available Cobre dataset (69 cases and 77 controls); see  
50 Methods. We mapped case-control MS differences at global  
51 and nodal levels of resolution individually in each dataset to  
52 assess replicability and we tested for significant differences  
53 in network organization that were consistent across studies.  
54 We used partial least squares (PLS) regression to test the  
55 hypothesis that this MRI network phenotype of psychosis was  
56 correlated with anatomically patterned gene expression using  
57 data from the Allen Human Brain Atlas (AHBA). This analyt-  
58 ical approach to combine imaging and genomic data has been  
59 methodologically established (5, 6) and applied in the context  
60 of neuropsychiatric disorders (7, 8). We used it to test the  
61 pathogenic hypothesis that the genes most strongly associated  
62 with case-control differences in MS were enriched: (i) for genes  
63 that have been ontologically linked to relevant neurobiological  
64 processes; and (ii) for genes that are abnormally expressed in  
65 post-mortem studies of schizophrenia.

## 66 Results

67 **Samples.** Socio-demographic and clinical data available on the  
68 sample are in Table S1. There was considerable heterogeneity  
69 in clinical measures between studies, e.g., the Maastricht pa-  
70 tients had relatively low mean scores on psychotic symptoms  
71 scales.

### 72 Case-control differences in global morphometric similarity.

73 Globally, MS was reduced in cases compared to controls in  
74 all 3 datasets (Fig. S2). Regional MS had an approximately  
75 Normal distribution over all 308 regions (after regressing age,  
76 sex and age  $\times$  sex) and in all 3 datasets there was a signif-  
77 icant case-control difference in this distribution ( $P < 0.001$ ,  
78 Kolmogorov-Smirnov test). Modal values of regional MS were  
79 more frequent, and extreme values less frequent, in cases com-  
80 pared to controls (Figs. 1a and S2).

### 81 Case-control differences in regional morphometric similarity.

82 The cortical map of regional MS in Fig. 1 c) summarises  
83 the anatomical distribution of areas of positive and negative  
84 similarity on average over controls from all 3 datasets. The  
85 results are similar to those reported in an independent sample  
86 (3), with high positive MS in frontal and temporal cortical  
87 areas and high negative MS in occipital, somatosensory and  
88 motor cortex. This confirms the replicability of this pattern  
89 of regional MS in healthy individuals and is consistent with  
90 prior knowledge that primary cortex is more histologically  
91 differentiated than association cortex.

92 We mapped the  $t$ -statistics and corresponding Hedge’s  $g$   
93 effect sizes for the case-control differences in regional MS at

each cortical area (Fig. 1 d). A positive  $t$ -statistic means  
MS increased in patients whereas a negative  $t$ -statistic means  
MS decreased. We found somewhat similar patterns of case-  
control difference across all 3 datasets, with increased regional  
MS in occipital and parietal areas in patients, and decreased  
regional MS in frontal and temporal cortex. The case-control  
 $t$ -map for the Dublin study was significantly correlated with  
both the Maastricht and the Cobre  $t$ -maps ( $r = 0.42$ ,  $P <$   
 $0.001$  and  $r = 0.47$ ,  $P < 0.001$ , respectively), although the  
Maastricht and Cobre  $t$ -maps were not significantly correlated  
( $r = 0.058$ ,  $P = 0.31$ ), see Fig. S4. However, a large number  
of patients in the Maastricht dataset had very low symptom  
scores (below the threshold for “borderline mentally ill” (9)). If  
those non-psychotic patients were excluded from the analysis,  
the Maastricht case-control  $t$ -map was correlated significantly  
with the Cobre map ( $r=0.22$ ,  $P < 0.001$ , see section S6.2).

Combining the  $P$ -values for case-control differences across  
all 3 datasets, we identified 18 cortical regions where MS was  
robustly and significantly different between groups (Fig. 1 e).  
MS decreased in patients in 15 regions located in the superior  
frontal, caudal middle frontal, pre-central, pars triangularis  
and superior temporal areas and increased in 3 regions located  
in superior parietal and post-central areas (Table S2).

To contextualise the regional MS case-control differences,  
we referred them to two prior classifications of cortical areas:  
the von Economo atlas of cortex classified by cytoarchitectonic  
criteria (5); and the Yeo atlas of cortex classified according  
to resting state networks derived from functional MRI (10,  
11). MS was significantly reduced in von Economo class 2  
(association cortex) and in the ventral attention, frontoparietal  
and default mode Yeo networks (all  $P_{FDR} < 0.05$ ; Tables S12  
and S13).

There was a strong negative correlation between regional  
MS in the control subjects and the case-control differences in  
regional MS (both averaged over all 3 datasets;  $P_{perm} = 0.002$ )  
(Fig. 1 f). Hence areas with highest positive MS in controls  
tended to show the greatest decrease of MS in patients; and,  
conversely, areas with highest negative MS in healthy controls  
had the greatest increase of MS in psychosis. This result  
is analogous to the observation that highly connected ‘hub’  
regions are the most likely to show reduced connectivity in  
disease in fMRI and DTI brain networks (12).

We tested for correlations between mean MS and a range  
of clinical measures, including symptom scores, anti-psychotic  
medication use and cannabis use, see section S6.3. The only sig-  
nificant associations after FDR correction were with cannabis  
use, which was positively correlated with mean global MS in  
the Maastricht study ( $P_{FDR} = 5 \times 10^{-4}$ ), as well as with mean  
MS averaged across the 15 regions with significantly decreased  
MS in Fig. 1e ( $P_{FDR}=0.0017$ ).

### Gene expression related to morphometric similarity.

We used PLS regression to identify patterns of gene expression that  
were correlated with the anatomical distribution of case-control  
MS differences. The first PLS component explained 13% of the  
variance in the case-control MS differences, combining data  
from all 3 studies, significantly more than expected by chance  
(permutation test,  $P < 0.001$ ). PLS1 gene expression weights  
were positively correlated with case-control MS differences in  
the Dublin study ( $r = 0.49$ ,  $P < 0.001$ ) and the Cobre study  
( $r = 0.37$ ,  $P < 0.001$ ) (Fig. 2a); but not in the Maastricht  
study ( $r = 0.006$ ,  $P = 0.94$ ). These positive correlations mean

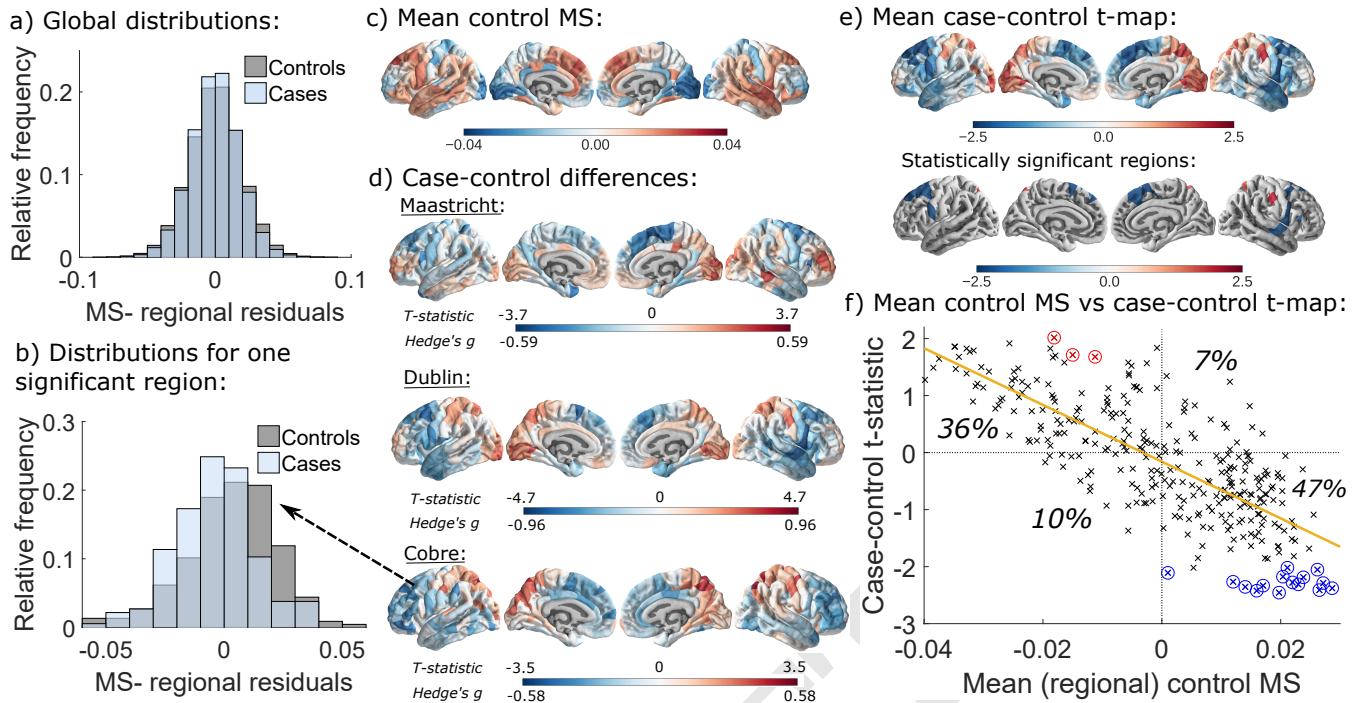


**Fig. 1. Case-control differences in regional MS.** a) Distributions of regional MS strength, i.e. the average similarity of each region to all other regions, for cases and controls from all datasets. b) Distributions of MS strength for a region with significantly reduced MS in cases, namely left hemisphere caudal middle frontal part 1. c) Regional MS averaged over controls from all 3 datasets. d) *t*-statistics and Hedge's *g* effect sizes for the case-control differences in regional MS in each dataset. e) *t*-statistics for regional case-control differences averaged across datasets in all regions and in the 18 cortical areas where the difference was statistically significant across datasets (FDR = 0.05). f) Scatterplot of mean control regional MS (*x*-axis) versus case-control *t*-statistic (*y*-axis). Control MS (from panel c) is strongly negatively correlated with case-control MS differences (from panel d) (Pearson's  $r = -0.76$ ,  $P < 0.001$ ). Most cortical regions have positive MS in controls which decreases in patients (47% of regions) or negative MS in controls which increases in patients (36% of regions). Statistically significant regions are circled in red/blue according to whether their mean *t*-statistic increases/decreases in patients.

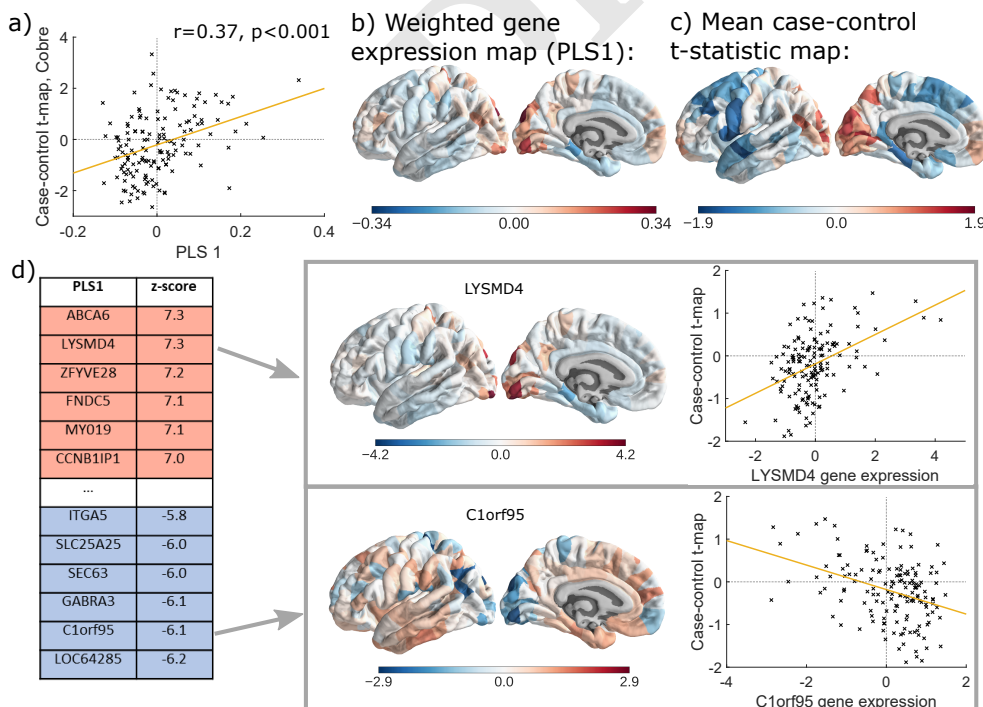


**Fig. 2. Gene expression profiles related to case-control differences in morphometric similarity.** a) Scatterplot of regional PLS1 scores (weighted sum of 20,647 gene expression scores) versus case-control differences in regional MS (Cobre dataset). b) Cortical map of regional PLS1 scores. c) Cortical map of mean case-control MS differences, averaged across all datasets. Here we include intra-hemispheric left hemisphere edges only (see Methods). d) Genes that are strongly positively weighted on PLS1 (e.g., *LYSM4*) correlate positively with case-control differences in regional MS ( $r = 0.44$ ,  $P < 0.001$ ); whereas genes that are strongly negatively weighted on PLS1 (e.g., *C1orf95*) correlate negatively with case-control differences in MS ( $r = -0.37$ ,  $P < 0.001$ ).

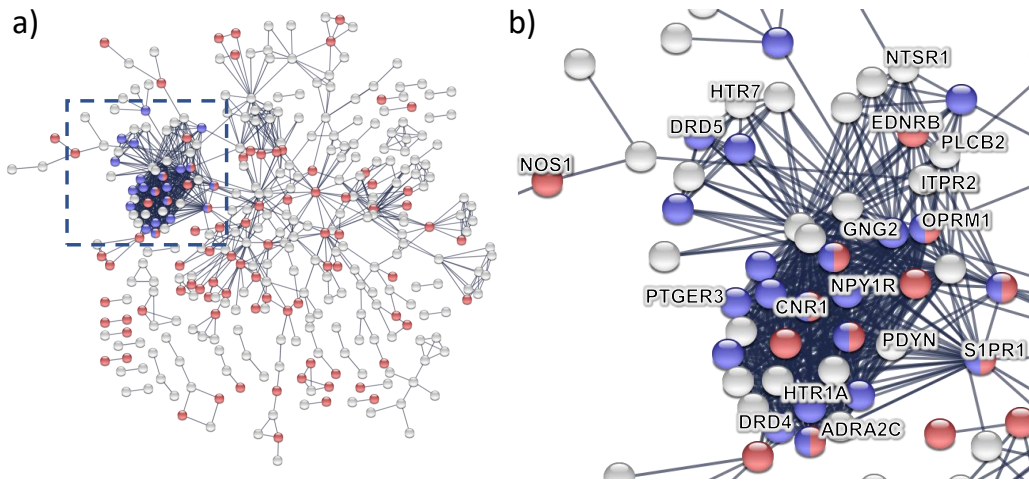


**Fig. 3. Enrichment analysis of genes transcriptionally related to morphometric similarity** a) protein-protein interaction (PPI) network for PLS- genes ( $Z < -3$ ), highlighted with some of the significantly GO enriched biological processes: “nervous system development” in red and “adenylate cyclase-modulating G-protein coupled receptor signaling pathway” in blue. The most interconnected set of proteins were coded by several genes previously implicated in schizophrenia, highlighted in part b). See the text and section S8.8 for details.

155 that genes positively weighted on PLS1 are over-expressed  
 156 in regions where MS was increased in patients, whilst negatively  
 157 weighted genes are over-expressed in regions where MS  
 158 was decreased in patients (Fig. 2d). Hence genes which are  
 159 positively (or negatively) weighted on PLS1 were related to  
 160 increased (or decreased) MS in cases compared to controls.

161 **Enrichment analysis of genes transcriptionally related to morphometric similarity.** We found 1110 genes with normalised  
 162 PLS1 weights  $Z < -3$ , which we denote the PLS- gene set,  
 163 and 1979 genes with  $Z > 3$ , which we denote the PLS+ gene  
 164 set. We first consider PLS- genes (the equivalent results for  
 165 PLS+ genes are also given below).  
 166

167 We mapped the network of known interactions between proteins  
 168 coded by the PLS- gene set (13) (Fig. 3). The resulting  
 169 protein-protein interaction (PPI) network had 341 connected  
 170 proteins and 1022 edges, significantly more than the 802 edges  
 171 expected by chance (permutation test,  $P < 1^{-13}$ ). We also  
 172 tested the PLS- gene set for significant GO enrichment of  
 173 biological processes and enrichment of KEGG pathways. Enriched  
 174 biological processes included “nervous system development”,  
 175 “synaptic signaling” and “adenylate cyclase-modulating  
 176 G-protein coupled receptor signaling pathway” (see Dataset  
 177 S1). There were two significantly enriched KEGG pathways:  
 178 “neuroactive ligand-receptor interaction” and “retrograde  
 179 endocannabinoid signaling” (Fig. S13). The proteins coded by  
 180 genes enriched for “adenylate cyclase-modulating G-protein  
 181 coupled receptor signaling pathway” and the two KEGG pathways  
 182 formed the most strongly inter-connected cluster of nodes  
 183 in the PPI network, see Fig. 3, compatible with them sharing  
 184 a specialised functional role for GPCR signaling.

185 Genes recently reported as over-expressed in post mortem  
 186 brain tissue from patients with schizophrenia (14) were highly  
 187 enriched among genes that were negatively weighted on PLS1  
 188 (permutation test,  $P < 0.001$ , after FDR correction). The  
 189 relationship between the sign of PLS1 weights of gene  
 190 expression related to the MRI case-control phenotype and the  
 191 sign of case-control differences in the histological measures of  
 192 brain gene expression was highly non-random (Wilcoxon rank  
 193 sum test,  $P < 10^{-26}$ ).

194 In other words, genes that were up-regulated in post mortem  
 195 brain tissue from patients with schizophrenia are normally  
 196 over-expressed in association cortical areas that have reduced MS in

197 psychosis. This association between gene expression in regions  
 198 with reduced MS and genes up-regulated in schizophrenia was  
 199 replicated by analysis of two alternative datasets provided by  
 200 the PsychENCODE consortium (15) and by (16), see section  
 201 S8.5. We also observed enrichment by genes up-regulated in  
 202 other psychiatric disorders, e.g., autistic spectrum disorders,  
 203 which is compatible with the substantial overlap between  
 204 genes which are up (or down) regulated in common between  
 205 schizophrenia and other neurodevelopmental disorders (15).

206 The PLS+ genes coded proteins that formed a PPI network  
 207 with significantly more edges than expected by chance ( $P < 10^{-6}$ ),  
 208 which was enriched for the biological process “nucleic acid  
 209 metabolic process” but no KEGG pathways, see Fig. S14.  
 210 Genes which are down-regulated post mortem in schizophrenia  
 211 (14) were highly enriched among genes that were positively  
 212 weighted on PLS1 (permutation test,  $P < 0.001$  after FDR  
 213 correction). This result was reproduced with genes reported  
 214 as down-regulated in schizophrenia by (16), although not by  
 215 the PsychENCODE consortium (15), see section S8.5.

216 There was no significant enrichment of PLS- or PLS+ genes  
 217 for common sequence variants associated with schizophrenia,  
 218 derived from a recent genome-wide association study (GWAS)  
 219 of PGC and CLOZUK samples (17) ( $P > 0.05$ ).

## 220 Discussion.

221 **Morphometric similarity network phenotypes.** Morphometric  
 222 similarity mapping disclosed a robust and replicable cortical  
 223 pattern of differences in psychosis patients. MS was significantly  
 224 reduced in frontal and temporal cortical areas, and significantly  
 225 increased in parietal cortical areas. This pattern was consistent  
 226 across 3 independent datasets, with different samples,  
 227 locations, scanners and scanning parameters.

228 What does this novel MRI phenotype of psychosis represent?  
 229 Morphometric similarity quantifies the correspondence or kin-  
 230 ship of two cortical areas in terms of multiple macro-structural  
 231 features, e.g., cortical thickness, and micro-structural features,  
 232 e.g., fractional anisotropy (FA), that are measurable by MRI.  
 233 We assume that high MS between a pair of cortical regions  
 234 indicates that there is a high degree of correspondence between  
 235 them in terms of cytoarchitectonic and myeloarchitectonic  
 236 features that we cannot directly observe, given the limited  
 237 spatial resolution and cellular specificity of MRI. Prior work  
 238 also showed that morphometrically similar cortical regions are

239 more likely to be axonally connected to each other, i.e., MS is  
240 a proxy marker for anatomical connectivity (3). We therefore  
241 interpret the reduced MS we observe in frontal and temporal  
242 brain regions in psychosis as indicating that there is reduced  
243 architectonic similarity, or greater architectonic differentiation,  
244 between these areas and the rest of the cortex, which is proba-  
245 bly indicative of reduced anatomical connectivity to and from  
246 the less similar, more differentiated cortical areas.

247 There is a well-evidenced and articulated prior theory of  
248 schizophrenia as a dysconnectivity syndrome, specifically func-  
249 tional dysconnectivity of frontal and temporal cortical areas  
250 has been recognised as a marker of brain network disorganiza-  
251 tion in schizophrenia (18). Our results of reduced MS in frontal  
252 and temporal cortex - implying increased architectonic differ-  
253 entiation and decreased axonal connectivity - are descriptively  
254 consistent with this theory. Our complementary finding of ab-  
255 normally increased MS in parietal cortex - implying increased  
256 architectonic similarity and axonal connectivity - is plausible  
257 but not so clearly precedented, given the relatively limited  
258 prior data on the parietal cortex in studies of schizophrenia  
259 as a dysconnectivity syndrome (19, 20).

260 Encouragingly, this novel MRI network marker of psychosis  
261 was highly reliable across three independent and method-  
262 ologically various case-control studies. This implies that the  
263 measurement is robust enough to be plausible as a candi-  
264 date imaging biomarker of cortical network organization in  
265 large-scale, multi-centre studies of psychosis.

266 **Transcriptional profiling of MS network phenotypes.** In an effort to  
267 connect these novel MRI phenotypes to the emerging genetics  
268 and functional genomics of schizophrenia, we first used partial  
269 least squares to identify the weighted combination of genes  
270 in the whole genome that has a cortical expression map most  
271 similar to the cortical map of case-control MS differences.  
272 Then we tested the mechanistic hypothesis that the genes  
273 with greatest (positive or negative) weight on PLS1 were  
274 enriched for genes previously implicated in the pathogenesis  
275 of schizophrenia.

276 We found that the genes that are normally over-expressed  
277 in frontal and temporal areas of reduced MS in psychosis,  
278 were significantly enriched for genes that are up-regulated in  
279 post mortem brain tissue from patients with schizophrenia  
280 (14). Conversely, the genes that are normally over-expressed  
281 in parietal and other areas of increased MS in psychosis were  
282 significantly enriched for genes that are down-regulated in post-  
283 mortem data (14). This tight coupling between MRI-derived  
284 transcriptional weights and gene transcription measured his-  
285 tologically was highly significant and replicated across three  
286 prior post-mortem datasets.

287 Further investigation showed that the proteins coded by  
288 the PLS- genes formed a dense, topologically clustered inter-  
289 action network that was significantly enriched for a number of  
290 relevant GO biological processes and KEGG pathways. The  
291 cluster of interactive proteins related to GPCR signaling in-  
292 cluded multiple proteins coded by genes previously linked to  
293 anti-psychotic mechanisms of action, including *DRD4* (21),  
294 *HTR1* (22), *NTSR1* (23) and *ADRA2C* (24); reported in  
295 transcriptional studies of post-mortem brain tissue, e.g., *PT-*  
296 *GER3*, *S1PR1*, *ITPR2* and *EDNRB* (14, 25); or associated  
297 with risk SNPs for schizophrenia, e.g. *DRD5*, *OPRM1* and  
298 *CNR1* (26–28). The remarkable density of therapeutically rel-  
299 evant genes in the GPCR-related cluster suggests that other,

300 topologically neighboring genes may deserve further attention  
301 as novel targets for anti-psychotic interventions.

302 Risk genes identified by the largest extant GWAS studies of  
303 schizophrenia were not significantly enriched among PLS- or  
304 PLS+ genes. Nevertheless, the involvement of PLS- genes fur-  
305 ther down the causal pathway is still mechanistically revealing  
306 and potentially useful.

307 **Methodological considerations.** Some limitations of this study  
308 should be highlighted. The whole brain data on “normal” brain  
309 tissue expression of the genome were measured post mortem in  
310 6 adult brains (mean age = 43 years) and not in age-matched  
311 subjects or patients with schizophrenia (such data are not  
312 currently available to our knowledge). Also, the transcriptional  
313 experiments we use to label genes as up- or down-regulated  
314 in schizophrenia were performed in regions of the parietal or  
315 prefrontal cortex (14), whereas the neuroimaging results are for  
316 the whole brain. We have used MRI data from 3 independent  
317 studies to measure MS networks but the studies used different  
318 scanning protocols, leading to estimation of morphometric  
319 similarity between regions on the basis of 7 MRI parameters  
320 that were measurable in all studies. Future work could usefully  
321 explore the opportunity to further improve sensitivity and  
322 reliability of the MS network biomarker of schizophrenia by  
323 optimising and standardising the MRI procedures to measure  
324 the most informative set of morphometric features. Finally,  
325 the datasets have varied, limited clinical information available,  
326 making it difficult to assess the clinical significance of the MS  
327 phenotype.

## 328 Materials and Methods 329

330 **Samples.** We used MRI data from 3 prior case-control studies: the  
331 Maastricht GROUP study (29) from the Netherlands; the Dublin  
332 dataset which was acquired and scanned at the Trinity College In-  
333 stitute of Neuroscience as part of a Science Foundation Ireland-funded  
334 neuroimaging genetics study (“A structural and functional MRI  
335 investigation of genetics, cognition and emotion in schizophrenia”);  
336 and the publicly available Cobre dataset (30). The Maastricht  
337 and Dublin datasets were PSYSCAN legacy datasets. All patients  
338 satisfied DSM-IV diagnostic criteria for schizophrenia or other non-  
339 affective psychotic disorders. MRI data were quality controlled for  
340 motion artifacts (section S1). The Euler number, which quantifies  
341 image quality (31), was not significantly different between groups  
342 in any of the studies but it was different between studies, indicating  
343 that the studies were ranked Dublin > Cobre > Maastricht in terms  
344 of image quality (Table S1).

345 **Morphometric similarity mapping.** The T1-weighted MRI data  
346 (MPRAGE sequence) and the diffusion-weighted imaging (DWI)  
347 data from all participants were pre-processed using a previously  
348 defined computational pipeline (5). Briefly, we used the recon-all  
349 (32) and trac-all (33) commands from FreeSurfer (version 6.0). Fol-  
350 lowing (3), the surfaces were then parcellated using an atlas with  
351 308 cortical regions, derived from the Desikan-Killiany atlas (5, 34).  
352 For each region, we estimated 7 parameters from the MRI and DWI  
353 data: grey matter volume, surface area, cortical thickness, Gaussian  
354 curvature, mean curvature, fractional anisotropy (FA) and mean  
355 diffusivity (MD). Each parameter was normalised for sample mean  
356 and standard deviation before estimation of Pearson’s correlation  
357 for each pair of Z-scored morphometric feature vectors, which were  
358 compiled to form a  $308 \times 308$  morphometric similarity matrix  $\mathcal{M}_i$   
359 for each participant,  $i = 1, \dots, N$  (3).

360 **Case-control analysis of MS networks.** The global mean MS for each  
361 participant is the average of  $\mathcal{M}_i$ . The regional mean  $MS_{i,j}$ , for the  
362  $i$ th participant at each region,  $j = 1, \dots, 308$ , is the average of the

363  $j$ th row (or column) of  $\mathcal{M}_i$ . For global and regional MS statistics  
 364 alike, we fit linear models to estimate case-control difference, with  
 365 age, sex, and age $\times$ sex as covariates. Our main results also replicated  
 366 in subsets of the data balanced for age and sex, see section S5.6.  
 367 P-values for case-control differences in regional MS were combined  
 368 across all 3 studies, using Fisher's method. The resulting P-value  
 369 for each region which was thresholded for significance using the false  
 370 discovery rate,  $FDR < 0.05$ , to control type 1 error over multiple  
 371 (308) tests.

372 **Transcriptomic analysis.** We used the AHBA transcriptomic dataset,  
 373 with gene expression measurements in 6 post-mortem adult brains  
 374 (35) (<http://human.brain-map.org>), aged 24-57. Each tissue sample  
 375 was assigned to an anatomical structure using the AHBA MRI  
 376 data for each donor (36). Samples were pooled between bilaterally  
 377 homologous cortical areas. Regional expression levels for each gene  
 378 were compiled to form a  $308 \times 20,647$  regional transcription matrix  
 379 (36). Since the AHBA only includes data for the right hemisphere  
 380 for two subjects, in our analyses relating gene expression to MRI  
 381 data we only consider intra-hemispheric left hemisphere edges (37).

382 We used PLS to relate the regional MS case-control differences  
 383 ( $t$ -statistics from the 152 cortical regions in the left hemisphere, cal-  
 384 culated from intra-left hemispheric edges only) to the post mortem  
 385 gene expression measurements for all 20,647 genes. PLS uses the  
 386 gene expression measurements (the predictor variables) to predict  
 387 the intra left hemisphere regional MS patient/control  $t$ -statistics  
 388 from all 3 datasets (the response variables). The first PLS com-  
 389 ponent (PLS1) is the linear combination of the weighted gene  
 390 expression scores that has a cortical expression map that is most  
 391 strongly correlated with the map of case-control MS differences.  
 392 The statistical significance of the variance explained by PLS1 was  
 393 tested by permuting the response variables 1,000 times. The error in  
 394 estimating each gene's PLS1 weight was assessed by bootstrapping  
 395 (resampling with replacement of the 308 cortical regions), and the  
 396 ratio of the weight of each gene to its bootstrap standard error was  
 397 used to calculate the Z-scores and hence rank the genes according  
 398 to their contribution to PLS1 (5).

399 We constructed PPI networks from the genes with PLS1 weights  
 400  $Z > 3$  and  $Z < -3$  (all  $P_{FDR} < 0.05$ ) using STRING version 10.5  
 401 (13). Our key results were robust to changing these thresholds to  
 402  $Z > 4$  and  $Z < -4$  (all  $P_{FDR} < 0.01$ ), see section S8.3. We used  
 403 DAVID (38, 39) to calculate enrichments of KEGG pathways and  
 404 GO enrichments of biological processes for genes with  $Z > 3$  or  
 405  $Z < -3$ , using a background gene list of 15,745 brain-expressed  
 406 genes, again see section S8.3 (37).

407 We used a resampling procedure to test for enrichment of PLS-  
 408 derived gene sets by genes previously associated with schizophrenia  
 409 by transcriptional data (14). The median rank of each risk gene set  
 410 in the PLS gene list was compared to the median rank of 10,000  
 411 randomly selected brain-expressed gene sets (3).

412 **Data and code availability.** All code and processed data used for the  
 413 analyses will be made available on GitHub on publication.

414 **ACKNOWLEDGMENTS.** This study was supported by grants  
 415 from the European Commission (PSYSCAN - Translating neuro-  
 416 imaging findings from research into clinical practice; ID: 603196)  
 417 and the NIHR Cambridge Biomedical Research Centre (Mental  
 418 Health). The Cobre data was downloaded from the Collaborative  
 419 Informatics and Neuroimaging Suite Data Exchange tool (COINS;  
 420 <http://coins.mrn.org/dx>) and data collection was performed at the  
 421 Mind Research Network, and funded by a Center of Biomedical Re-  
 422 search Excellence (COBRE) grant 5P20RR021938/P20GM103472  
 423 from the NIH to Dr. Vince Calhoun. SEM holds a Henslow Fellow-  
 424 ship at Lucy Cavendish College, University of Cambridge, funded  
 425 by the Cambridge Philosophical Society. PEV was supported by the  
 426 Medical Research Council (MR/K020706/1) and an MQ fellowship  
 427 (MQF17\_24) and is a Fellow of the Alan Turing Institute funded  
 428 under the EPSRC grant EP/N510129/1. KJW was funded by an  
 429 Alan Turing Institute Research Fellowship under EPSRC Research  
 430 grant TU/A/000017. ETB is supported by a NIHR Senior Investi-  
 431 gator Award. The views expressed are those of the author(s) and  
 432 not necessarily those of the NHS, the NIHR or the Department of  
 433 Health and Social Care.

1. Wright I, et al. (2000) Meta-analysis of regional brain volumes in schizophrenia. *Am J Psychiatry* 157:16–25. 434

2. Alexander-Bloch A, Giedd J, Bullmore E (2013) Imaging structural co-variance between hu- 435  
man brain regions. *Nature Reviews Neuroscience* 14:322–336. 436

3. Seidlitz J, et al. (2018) Morphometric similarity networks detect microscale cortical organisa- 437  
tion and predict inter-individual cognitive variation. *Neuron* 97:231–247. 438

4. Goulas A, Uylings H, Hilgetag C (2017) Principles of ipsilateral and contralateral cortico- 439  
cortical connectivity in the mouse. *Brain Structure and Function* 222:1281–1295. 440

5. Whitaker K, et al. (2016) Adolescence is associated with genomically patterned consolidation 441  
of the hubs of the human brain connectome. *PNAS* 113:9105–9110. 442

6. Vértes P, et al. (2016) Gene transcription profiles associated with inter-modular hubs and con- 443  
nection distance in human functional magnetic resonance imaging networks. *Philosophical 444  
Transactions of the Royal Society B* 371:1705. 445

7. McColgan P, et al. (2017) Brain regions showing white matter loss in Huntington's disease 446  
are enriched for synaptic and metabolic genes. *Biological Psychiatry* 83:456–465. 447

8. Romero-García R, Warrier V, Bullmore E, Baron-Cohen S, Bethlehem R (2018) Synaptic and 448  
transcriptionally downregulated genes are associated with cortical thickness differences in 449  
autism. *Mol Psychiatry*. 450

9. Leucht S, et al. (2005) What does the PANSS mean? *Schizophrenia Research* 79:231–238. 451

10. Yeo BT, et al. (2011) The organization of the human cerebral cortex estimated by intrinsic 452  
functional connectivity. *Journal of Neurophysiology* 106(3):1125–1165. 453

11. Váša F, et al. (2018) Adolescent tuning of association cortex in human structural brain net- 454  
works. *Cerebral Cortex* 28:281–294. 455

12. Crossley N, et al. (2014) The hubs of the human connectome are generally implicated in the 456  
anatomy of brain disorders. *Brain* 137:2382–2395. 457

13. Szklarczyk D, et al. (2017) The STRING database in 2017: quality-controlled protein-protein 458  
association networks, made broadly accessible. *Nucleic Acids Res.* 45:362–368. 459

14. Gandal M, et al. (2018) Shared molecular neuropathology across major psychiatric disorders 460  
parallels polygenic overlap. *Science* 359:693–697. 461

15. Gandal M, et al. (2018) Transcriptome-wide isoform-level dysregulation in ASD, schizophre- 462  
nia, and bipolar disorder. *Science* 362:6420. 463

16. Fromer M, et al. (2016) Gene expression elucidates functional impact of polygenic risk for 464  
schizophrenia. *Nature Neuroscience* 19:1442–1453. 465

17. Pardiñas A, et al. (2018) Common schizophrenia alleles are enriched in mutation-intolerant 466  
genes and in regions under strong background selection. *Nat. Genet.* 50:381–389. 467

18. Friston K, Frith C (1995) Schizophrenia: a disconnection syndrome. *Clin Neurosci* 3:89–97. 468

19. Zhou SY, et al. (2007) Parietal lobe volume deficits in schizophrenia spectrum disorders. 469  
*Schizophrenia Research* 89:35–48. 470

20. Yildiz M, Borgwardt S, Berger G (2011) Parietal lobes in schizophrenia: Do they matter? 471  
*Schizophr Res Treatment* 2011:581686. 472

21. Xu F, Wu X, Zhang J, Wang B, Yao J (2018) A meta-analysis of data associating DRD4 473  
gene polymorphisms with schizophrenia. *Neuropsychiatr Dis Treat.* 14:153–164. 474

22. Røellema H, Lu Y, Schmidt A, Sprouse J, Zorn S (2000) 5-HT1A receptor activation contributes 475  
to ziprasidone-induced dopamine release in the rat prefrontal cortex. *Biol. Psychiatry* 48:229– 476  
237. 477

23. Austin J, et al. (2000) The high affinity neurotensin receptor gene (NTSR1): comparative 478  
sequencing and association studies in schizophrenia. *Molecular Psychiatry* 5:552–557. 479

24. Feng J, et al. (2001) An in-frame deletion in the alpha(2C) adrenergic receptor is common in 480  
African-Americans. *Mol. Psychiatry* 6:168–72. 481

25. Tang B, Capitaio C, Dean B, Thomas E (2012) Differential age- and disease-related effects on 482  
the expression of genes related to the arachidonic acid signaling pathway in schizophrenia. 483  
*Psychiatry Res.* 196:201–206. 484

26. Zhao Y, Ding M, Pang H, Xu X, Wang B (2014) Relationship between genetic polymorphisms 485  
in the DRD5 gene and paranoid schizophrenia in northern Han Chinese. *Genetics and Molecu- 486  
lar Research* 13:1609–1618. 487

27. Serý O, Prikryl R, Castulík L, St'astný F (2010) A118G polymorphism of OPRM1 gene is 488  
associated with schizophrenia. *J Mol Neurosci.* 41:219–222. 489

28. Gouvêa E, et al. (2017) The role of the CNR1 gene in schizophrenia: a systematic review 490  
including unpublished data. *Braz J Psychiatr* 39:160–171. 491

29. Habets P, et al. (2011) Reduced cortical thickness as an outcome of differential sensitivity to 492  
environmental risks in schizophrenia. *Biological Psychiatry* 69:487–494. 493

30. Çetin M, et al. (2014) Thalamus and posterior temporal lobe show greater inter-network con- 494  
nectivity at rest and across sensory paradigms in schizophrenia. *NeuroImage* 97:117–126. 495

31. Rosen A, et al. (2017) Quantitative assessment of structural image quality. *NeuroImage* 496  
169:407–418. 497

32. Dale A, Fischl B, Sereno M (1999) Cortical surface-based analysis. I. Segmentation and 498  
surface reconstruction. *NeuroImage* 9:179–194. 499

33. Yendiki A, et al. (2011) Automated probabilistic reconstruction of white-matter pathways in 500  
health and disease using an atlas of the underlying anatomy. *Front. Neuroinform.* 5:23. 501

34. Romero-García R, Atienza M, Clemmensen L, Cantero J (2012) Effects of network resolution on 502  
topological properties of human neocortex. *NeuroImage* 59:3522–3532. 503

35. Hawrylycz M, et al (2012) An anatomically comprehensive atlas of the adult human brain 504  
transcriptome. *Nature* 489:391–399. 505

36. Romero-García R, et al. (2018) Structural covariance networks are coupled to expression of 506  
genes enriched in supragranular layers of the human cortex. *NeuroImage* 171:256–267. 507

37. Arnatkeviciute A, Fulcher B, Fornito A (2018) A practical guide to linking brain-wide gene 508  
expression and neuroimaging data. *NeuroImage* 189:353–367. 509

38. Huang D, Sherman B, Lempicki R (2009) Systematic and integrative analysis of large gene 510  
lists using DAVID bioinformatics resources. *Nature Protoc.* 4:44–57. 511

39. Huang D, Sherman B, Lempicki R (2009) Bioinformatics enrichment tools: paths toward the 512  
comprehensive functional analysis of large gene lists. *Nucleic Acids Res.* 37:1–13. 513